Proc. SPIE, Vol.8440 (2012) 844009-1 ~ 844009-10 [10 pages]

Realization and application of strong coupling of single cesium atoms with TEM_{00} and TEM_{10} modes of a high-finesse Fabry-Perot cavity

Junmin Wang*, Pengfei Zhang, Gang Li, Tiancai Zhang**
State Key Laboratory of Quantum Optics and Quantum Optics Devices of China (Shanxi University), and Institute of Opto-Electronics, Shanxi University,
92 Wu Cheng Road, Taiyuan 030006, Shanxi Province, P. R. China

ABSTRACT

Strong coupling of single cesium atoms with a high-finesse optical micro-cavity (the finesse of our Fabry-Perot-type micro-cavity is $F = 3.3 \times 10^5$ and the cavity length is $l_c = 86$ μm) has been realized for the both cases of TEM_{00} and TEM_{10} cavity modes in our experiments. The typical parameters are $(g_{00}, \kappa, \gamma) = 2\pi \times (23.9, 2.6, 2.6)$ MHz and $(g_{10}, \kappa, \gamma) = 2\pi \times (20.5, 2.6, 2.6)$ MHz for these two cases, respectively. Obviously our system reaches the strong coupling regime. The first application is to adopt strong coupling of free-fall individual atoms with the TEM_{00} cavity mode for determining the effective temperature of laser-cooled atoms prepared in a magneto-optical trap located just above the micro-cavity. The second application is to employ strong coupling of free-fall individual atoms with the tilted TEM_{10} cavity mode, in stead of TEM_{00} mode, for more precisely tracking the trajectories of atoms passing through the cavity mode.

Keywords: Cavity QED, single atoms, high-finesse micro-cavity, strong coupling, TEM_{00} cavity mode, TEM_{10} cavity mode, effective temperature of cold atoms, atomic trajectory

1. INTRODUCTION

Laser cooling and trapping neutral atoms [1] becomes an efficient tool with which people can prepare cold atomic sample even single atoms and finds more and more important applications. This tool makes it possible to further fully control the external and internal freedom degree of cold atoms. Cavity quantum electrodynamics (cavity QED) [2] provides a nice playground for near deterministically controlling the atom-photon interaction on single-photon and single-atom level. Since the laser cooling and trapping married with the cavity QED more and more important progresses have been achieved [3-5]. If the coupling factor between atom and cavity mode is larger than the cavity field decay rate and the transverse atomic dipole decay rate it reach the strong coupling regime [2]. In this case even only one atom or one photon entering into or escaping from the cavity mode will completely modify the state of whole atom-cavity system. So the strong coupling cavity QED can be utilized to explore the statistic characteristics of atoms by counting atoms [6] and to detect single atoms [7-9].

Employing a horizon-oriented high-finesse Fabry-Perot(FP)-type micro-cavity and a cesium (Cs) magneto-optical trap (MOT) just 5 mm above the micro-cavity we realized the strong coupling of individual atoms with either TEM_{00} mode or TEM_{10} mode of the cavity. We adopted the strong coupling of free-fall individual atoms with the TEM_{00} cavity mode [10] for determining the effective temperature of laser-cooled atoms in the MOT. In this application the high-finesse FP-type micro-cavity actually acts as an atom detector [5] to determine the arrival times of individual freely falling atoms released from the MOT passing through the cavity mode, further the initial effective temperature of cold atoms in the MOT can be derived from the atomic velocity statistics. Obviously this is an alternative method for measuring the cold atoms' effective temperature, in stead of the conventional temperature determining methods, such as the release and recapture (R&R) [11, 12], the time of flight (TOF) [12], the trap-by-trap centre oscillation [13], the 2D TOF imaging [14], the transient four-wave mixing [15], the short-distance TOF [16-18], and the 1D R&R [19].

---

* **Corresponding author, wwjjmm@sxu.edu.cn; Phone: +86-351-7011844; Fax: +86-351-7011500**
** **Corresponding author, tczhang@sxu.edu.cn; Phone: +86-351-7011004; Fax: +86-351-7011500**

Quantum Optics II, edited by Thomas Durt, Victor N. Zadkov, Proc. of SPIE Vol. 8440, 844009 · © 2012 SPIE · CCC code: 0277-786X/12/$18 · doi: 10.1117/12.922110

We also employ the strong coupling of individual atoms with the ~45-degree-tilted TEM_{10} cavity mode for more precisely tracking the trajectories of individual atoms, which freely fall and vertically pass through the anti-node plane of the micro-cavity [20]. Thanks to the ~45-degree-tilted TEM_{10} cavity mode, in stead of TEM_{00} mode, the degeneracy for determining atomic trajectories is eliminated. This allows us to more precisely determine individual atom's vertical trajectory along the off-axis horizontal direction. Typical spatial resolution of ~ 0.1 μm is achieved in a measurement time of ~ 10 μs, and it is much better than previous measurements [21, 22].

2. STRONG COUPLING OF INDIVIDUAL ATOMS WITH THE MICRO-CAVITY

Our cavity QED experimental system is schematically depicted in Figure 1. The optical FP-type micro-cavity is formed by two tapered super-mirrors with spherical radius of 10 cm and ultra-high reflectivity around 852nm, and placed inside a no-magnet stainless-steel ultrahigh-vacuum chamber. The measured cavity length is l_c = 86 μm. The measured finesse of the micro-cavity is $F = 3.3 \times 10^5$. During the following experiments the micro-cavity is actively stabilized by using the lock laser at 828 nm which is another longitudinal mode of the cavity via the transfer cavity technique, in this way the frequency detuning between the cavity and the atomic transition (Cs $6S_{1/2}$ F = 4 - $6P_{3/2}$ F' = 5 cycling transition) Δ_{ca} can be controlled. Cs atoms are cooled and trapped in a vapor-cell MOT located 5 mm just above the micro-cavity. When the MOT is switched off some of the cold atoms will freely fall and pass through the cavity mode due to gravity. The mean dwelling time of free-fall atoms inside the TEM_{00} cavity mode is determined at ~ 120 μs. The frequency detuning between the probe laser beam and the atomic transition (Cs F = 4 - F' = 5 cycling transition) Δ_{pa} also can be precisely controlled independently, is injected into the micro-cavity. Transmitted photons from the cavity are separated with the 828-nm lock laser via a polarization-beam-splitter cube (PBS) and then counted by an avalanche photodiode (APD) (SPCM-14, Perkin Elmar) working in the photon-counting mode with a quantum efficiency of ~ 50% at 852 nm.

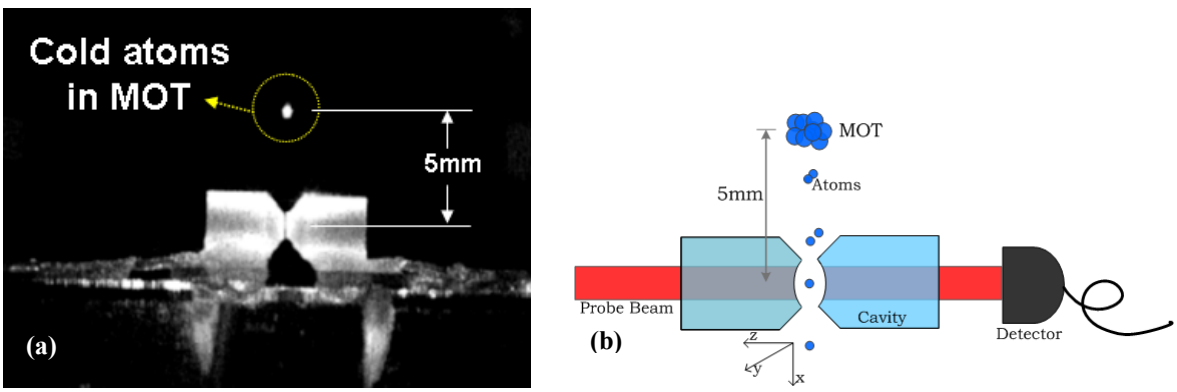

Figure 1. (Color online) Photo **(a)** and schematic diagram **(b)** of our cavity-QED system. About 10^5 Cs atoms were cooled and trapped in the MOT which is located 5 mm above the FP-type micro-cavity with a finesse $F = 3.3 \times 10^5$ and the cavity length l_c = 86 μm. The coordinates are chosen as labeled in **(b)**. The cavity center is reasonably chosen for ($x = 0$, $y = 0$, $z = 0$), here x along the gravity direction, z long the cavity axis.

The interaction between individual atoms and the cavity mode can be simply described by the well-known Jaynes–Cummings model. The vacuum Rabi splitting is measured and compared with the theoretical prediction. The results are shown in Figure 2. The typical parameters are $(g_{00}, \kappa, \gamma) = 2\pi \times (23.9, 2.6, 2.6)$ MHz, here $g_{00} = 2\pi \times 23.9$ MHz is the coupling factor of the TEM_{00} cavity mode with individual atoms, and it is much larger than the cavity field decay rate ($\kappa = 2\pi \times 2.6$ MHz) and the transverse atomic dipole decay rate ($\gamma = 2\pi \times 2.6$ MHz), thus our system obviously reaches the strong coupling regime ($g_{00} > \kappa, g_{00} > \gamma$). The typical parameters for the TEM_{10} cavity mode are $(g_{10}, \kappa, \gamma) = 2\pi \times (20.5, 2.6, 2.6)$ MHz, and it is still in the strong coupling regime.

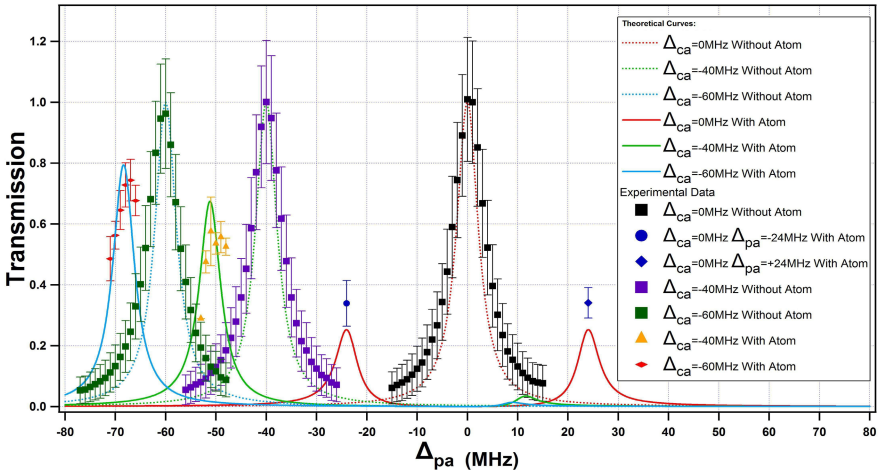

Figure 2. (Color online) The measured transmission signals versus the frequency detuning between the probe laser and the atomic transition (Cs $6S_{1/2}$ F = 4 – $6P_{3/2}$ F' = 5 cycling transition) and the theoretical predictions. Clearly the vacuum Rabi splitting is observed. The typical parameters are $(g_{00}, \kappa, \gamma) = 2\pi \times (23.9, 2.6, 2.6)$ MHz.

3. MEASUREMENT OF THE EFFECTIVE TEMPERATURE OF COLD ATOMS

We employed the strong coupling of free-fall individual Cs atoms released from the MOT with the TEM_{00} cavity mode to determine the effective temperature of clod atoms in the MOT [10].

Velocity distribution of cold atoms in the MOT follows the Maxwell-Boltzmann distribution, which can be expressed as following:

$$N(v)\cdot d^3v = (\frac{M}{2\pi k_B T})^{3/2}\cdot \exp[-\frac{M(v_x^2+v_y^2+v_z^2)}{2k_B T}]\cdot d^3v \qquad (1)$$

here M stands for the atomic mass, k_B = 1.38 x 10^{-23} J/K is the Boltzmann constant, T is the effective temperature of cold atom, and v_i ($i = x, y, z$) are the components of the root-mean-square (rms) velocity of cold atoms along the x, y and z directions. The vertical distance between the MOT center and the cavity center is h, so that the coordinates for the MOT center are ($x_{MOT} = h$, $y_{MOT} = 0$, $z_{MOT} = 0$). In order to obtain the probability distribution of the arrival times of atoms reaching the cavity, the rms velocity components (v_x, v_y, v_z) in equation (1) should be transformed to the coordinates (x, y, z). After the cold atoms are released from the MOT at the time t = 0, at the time t the coordinates ($x(t)$, $y(t)$, $z(t)$) of the center of the cold cloud should read:

$$x(t) = v_x t + \tfrac{1}{2}gt^2 - h, \qquad y(t) = v_y t, \qquad z(t) = v_z t \qquad (2)$$

here g = 9.8 m/s^2 is the gravitational acceleration.

After rewriting (2) we can get:

$$v_x = [x(t) - \tfrac{1}{2}gt^2 + h]/t, \qquad v_y = y(t)/t, \qquad v_z = z(t)/t \qquad (2A)$$

In this way the rms velocity components (v_x, v_y, v_z) can be substituted by ($x(t)$, $y(t)$, $z(t)$). The term d^3v in equation (1) should be transformed to $dydzdt$ by using the Jacobian transform.

In the y-z plane, the area of the micro-cavity TEM_{00} mode is approximately ($2w_0$ x l_c) = (47.6 μm x 86 μm), where w_0 = 23.8 μm is the waist radius of the TEM_{00} cavity mode and l_c = 86 μm is the cavity length. The vertical distance between the MOT center and the cavity center is h = 5mm, which is very short distance but is much larger than the size of the micro-cavity TEM_{00} mode. Thus we can approximately regard the micro-cavity as a point. Finally we get the time

dependent probability $P(t)$ for individual atoms arriving at the micro-cavity as following [10]:

$$P(t) \propto (\frac{M}{2\pi k_B T})^{3/2} \cdot \frac{\frac{1}{2}gt^2 + h}{t^4} \cdot \exp[-\frac{M(\frac{1}{2}gt^2 - h)^2}{2k_B T t^2}] \quad (3)$$

Because the cavity transmission signal is quite sensitive to the atom arrival at the micro-cavity mode due to the strong coupling of individual atoms with the micro-cavity, we can adopt the micro-cavity to count the arrival time of free-fall cold atoms. This is really a kind of "atom detector" [6-9]. To measure atom-arriving times, the micro-cavity and the probe laser are both controlled to resonate with the Cs F = 4 - F' = 5 cycling transition ($\Delta_{ca} \sim 0$, $\Delta_{pa} \sim 0$). The typical transmission signals from the micro-cavity detected by the APD with and without atom arrivals are shown in Figure 3.

This measurement is repeated many times with the same initial parameters of the MOT to obtain the probability distribution of individual atoms arrival at the micro-cavity. The initial effective temperature of cold atoms in the MOT can be derived from the fitting to the measured data of atom-arriving times by the above-mentioned model. Figure 4(a) shows the probability distribution of individual atoms arrival times based on total 664 atom-detection events. From data fitting (the dashed line in Figure 4(a)) we derived that the initial effective temperature of cold atoms in the MOT, T = 256 μK ± 3 μK, which is much higher than the Doppler cooling limit (~125 μK for Cs atoms). For this case the initial experimental parameters of the MOT are kept as follow: the total intensity of the cooling laser beams is ~ 12.5 mW/cm^2, the frequency detuning between the cooling laser and the Cs F = 4 - F' = 5 cycling transition is ~ -12 MHz, the total intensity of the repumping laser beams which is resonate with the Cs F = 3 - F' = 4 transition is ~ 9.4 mW/cm^2, the quadrupole magnetic gradient of MOT magnetic filed is ~ 9.2 Gauss/cm, typical pressure inside the vacuum chamber is ~ 3 x 10^{-10} Torr, and total cold atoms number is ~ 1 x 10^5.

After changing the experimental parameters of the MOT (decreases the total intensity of the cooling laser beams at ~ 8.8 mW/cm^2 and the total intensity of the repumping laser beams at ~ 8.2 mW/cm^2, the detuning of the cooling laser is set at -10 MHz), we have done another set of measurements. The results are shown in Figure 4(b). Now the initial effective temperature is ~ T = 117 μK ± 8 μK, which is lightly lower than the Doppler cooling limit for Cs (~125 μK). Here we noted that no optimization of the MOT parameters is made further although the effective temperature of cold atoms is high.

Besides the conventional methods for measuring the effective temperature of cold atoms [12-20], which are mentioned in the INTRODUCTION part, this is an alternative method. The advantage is that it works well even for a very small number of cold atoms.

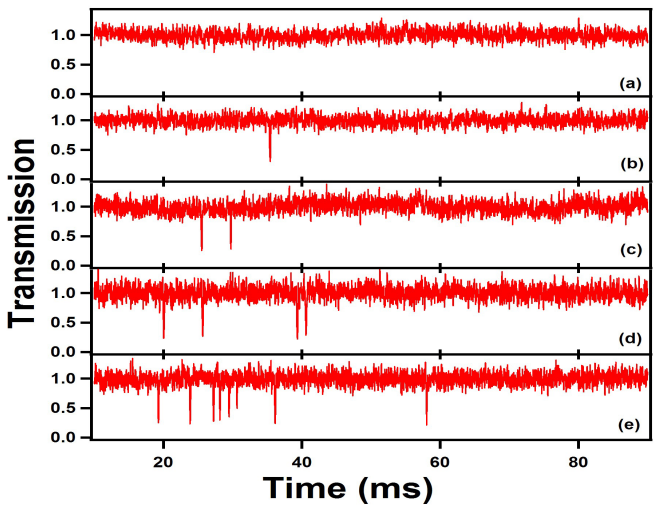

Figure 3. (Color online) Typical transmission signals from the high-finesse micro-cavity without and with atom arrivals. (a)-(e) stands for the cases of 0, 1, 2, 4, and 8 detection events for atom arriving at the cavity.

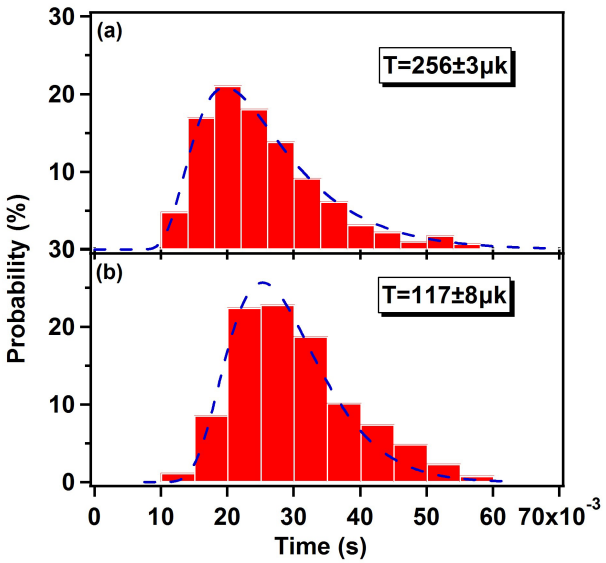

Figure 4. (Color online) Measured probability distribution for individual free-fall atoms arrival at the micro-cavity and the corresponding theoretical fittings. **(a)** and **(b)** stand the different two sets of initial experimental parameters of the MOT. The errors come from the statistical error of the fitting.

4. DETERMINATION OF THE TRAJECTORY OF INDIVIDUAL ATOMS PASSING THROUGH THE MICRO-CAVITY

The strong coupling of individual atoms with the TEM_{00} cavity mode also can be employed to determine the trajectory of single atom. In 2000, by employing the strong coupling of single atoms with the TEM_{00} cavity mode, Hood *et al* [21] tracked and reconstructed the 2D trajectories of single atom which was trapped in the standing-wave optical dipole trap inside a high-finesse micro-cavity. They showed that trapped atom moved randomly in elliptical orbits in the antinode plane which is perpendicular to the cavity axis and ~ 2 μm of the spatial resolution in 10 μs time was achieved for determining 2D trajectories of single atoms [21].

In our case, we do not have the optical dipole trap inside the micro-cavity. When cold atoms are released from the MOT, some atoms with only v_x and small v_y components (but $v_z = 0$) will freely fall and pass through the cavity mode. So the motional trajectories of individual atoms which pass through the cavity mode are almost straight lines along the gravity direction. Because the vertical distance between the MOT center and the cavity center (h = 5 mm) is ~ 60 times larger than the length of the micro-cavity (l_c = 86 μm), after releasing from the MOT the atoms with a non-zero v_z component in initial velocities will have horizontal displacement along the cavity axis, thus they can not pass through the cavity. Of course the probe laser's intensity inside the cavity should be very weak, thus it almost does not perturb the passing atoms' trajectories.

When ignoring the intra-cavity atomic motion along the cavity axis (z direction), and assuming the free-fall atoms pass through the cavity mode near the antinode, the 2D expression of the cavity transmission after atom-cavity interaction is as follows [11]:

$$T(x',y') = \frac{\kappa^2(\gamma^2+\Delta_{pa}^2)}{[g_{eff}^2(x',y') - \Delta_{pa}^2 + \Delta_{ca}\cdot\Delta_{pa} + \gamma\cdot\kappa]^2 + (\kappa\cdot\Delta_{pa} + \gamma\cdot\Delta_{pa} - \gamma\cdot\Delta_{ca})} \tag{4}$$

here $g_{eff}(x', y') = g_0\Psi_{m,n}(x', y')/\Psi_{0,0}(0, 0)$ is the effective coupling factor for the TEM_{mn} Hermite-Gaussian transverse cavity mode, where $\Psi_{m,n}(x', y') = (m!n!2^m2^n)^{-1/2}(\pi w_0^2/2)^{-1/2}\exp[-(x'^2+y'^2)/w_0^2]H_m(2^{1/2}x'/w_0)H_n(2^{1/2}y'/w_0)$ is the TEM_{mn}

mode function, $H_{m,n}$ is the Hermite polynomial of the order m and n, w_0 is the waist radius of the mode, Δ_{pa} is the frequency detuning between the probe laser beam and the atomic transition, and Δ_{ca} is the frequency detuning between the micro-cavity and the atomic transition. The x'-y' plane is perpendicular to the z direction, but x' and y' are chosen along the nodal lines of the TEM_{mn} mode. Considering the TEM_{10} mode, the nodal line between two lobes may along any direction. If θ is used to indicate the angle between the nodal line and x direction, a rotating coordinate transform should be used as follows:

$$x' = x \cdot \cos\theta - y \cdot \sin\theta, \qquad y' = x \cdot \sin\theta + y \cdot \cos\theta \tag{5}$$

If considering the TEM_{00} cavity mode, we have $m = n = 0$, the mode function is simplified to $\Psi_{0,0}(x', y') = g_0 \exp[-(x'^2+y'^2)/w_0^2] = g_0 \exp[-(x^2+y^2)/w_0^2]$.

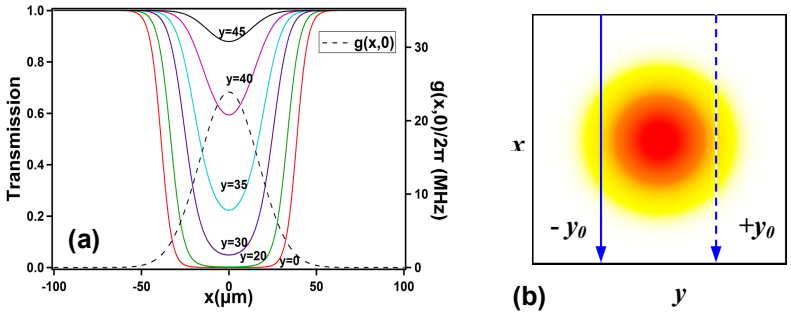

Figure 5. (Color online) If the single atom's trajectories with which the atom passing through the cavity mode are determined by employing the TEM_{00} cavity mode (as shown in **(b)**), the transmission signals are calculated for different trajectories (y = 0, ± 20 μm, ± 30 μm, ± 35 μm, ± 40 μm, and ± 45 μm), as shown in **(a)**. Obviously it has duplicate degeneracy.

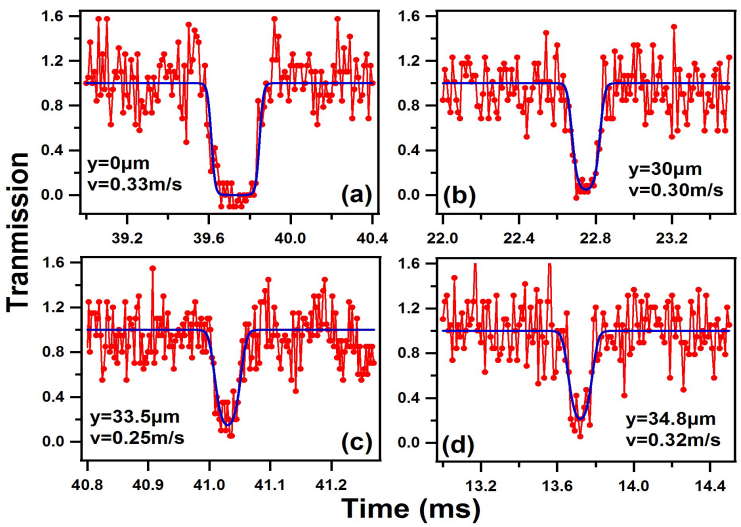

Figure 6. (Color online) Our typical results of the single atom's trajectories which are determined by employing the TEM_{00} cavity mode. The red dots are measured signals, and the blue solid lines are the theoretical fittings. **(a)** for the trajectory $y \sim 0$; **(b)** for the trajectories $y \sim \pm 30$ μm; **(c)** for the trajectories $y \sim \pm 33.5$ μm; **(d)** for the trajectories $y \sim \pm 34.8$ μm. Further more the atomic velocity component v_x can be derived.

The cavity transmission given by expression (4) is position dependent, thus the atomic trajectory can be determined by theoretical fitting the measured cavity transmission spectrum in which x is connected with the atomic arrival time t (see equation (2)). We calculated the cavity transmission spectra for the TEM_{00} cavity mode (as shown in Figure 5(b)). The calculation results are depicted in Figure 5(a). Obviously each transmission signal may corresponds to two different trajectories ($\pm y_0$), except the case for $y = 0$, so it has duplicate degeneracy. It seems that the TEM_{00} cavity mode is not a best choice for determining the atomic trajectory. The experimental results for using the TEM_{00} cavity mode are shown in Figure 6. The theoretical fittings by expression (4) have been done to get possible atomic trajectories.

Now let's switch to the case of the TEM_{10} cavity mode. Figure 7(c) and (d) show the intensity distributions for the horizon-oriented TEM_{10} mode and the vertical-oriented TEM_{01} mode. In 2004, Puppe *et al* [22] determined the atomic trajectories inside a high-finesse cavity by employing the strong coupling of single atoms with the TEM_{10} mode with a vertical-oriented nodal line or the TEM_{01} mode with a horizon-oriented nodal line of their cavity. Their results are sited here, as sketched in Figure 7(a) and (b). The cavity transmission spectrum shown in Figure 7(a) corresponds to one of the four different trajectories ($\pm y_1$ and $\pm y_2$), as indicated by the four lines with arrows in Figure 7(c), thus it has fourfold degeneracy. Also the cavity transmission spectrum shown in Figure 7(b) corresponds to one of the two different trajectories ($\pm y_0$), as indicated by the two lines with arrows in Figure 7(d), thus it has duplicate degeneracy. It seems that the TEM_{10} mode with a vertical-oriented nodal line and the TEM_{01} mode with a horizon-oriented nodal line are also not best choice for determining the atomic trajectory.

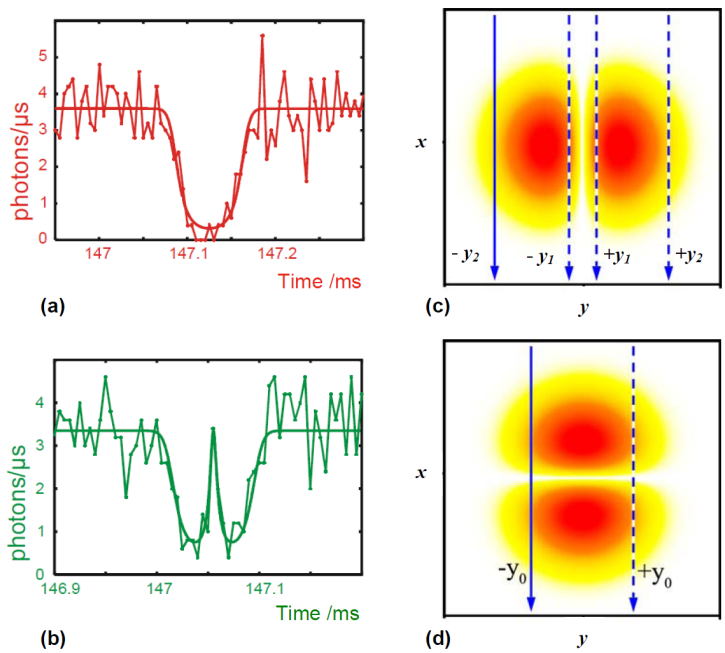

Figure 7. (Color online) The single atom's trajectories with which the atom passing through the cavity mode are determined by employing the TEM_{10} cavity mode with a vertical-oriented nodal line (as shown in **(c)**) and the TEM_{01} cavity mode with a horizon-oriented nodal line (as shown in **(d)**). The results of Puppe *et al* (ref. [22]) are shown in **(a)** for the cavity mode **(c)**, and **(b)** for the cavity mode **(d)**. Obviously result **(a)** corresponds to one of the four different trajectories ($\pm y_1$ and $\pm y_2$), so it has fourfold degeneracy; also result **(b)** corresponds to one of the two different trajectories ($\pm y_0$), so it has duplicate degeneracy.

Now we consider the case with the tilted TEM_{10} cavity mode. In principle, the fourfold degeneracy in the case of the TEM_{10} mode with a vertical-oriented nodal line (see Figure 7(b)) and the duplicate degeneracy in the case of the TEM_{01} mode with a horizon-oriented nodal line (see Figure 7(d)) will be eliminated completely because the mode symmetry is broken. Fortunately, our high-finesse micro-cavity has ~ 45-degree-tilted TEM_{10} and TEM_{01} modes, as

shown in Figure 8. The frequency splitting between the TEM_{10} and TEM_{01} modes is ~ 82.5 MHz, so it is very easy to distinguish them. In our experiment, we chose the tilted TEM_{10} cavity mode because it is stronger than the tilted TEM_{01} cavity mode. The typical parameters for this case are $(g_{10}, \kappa, \gamma) = 2\pi \times (20.5, 2.6, 2.6)$ MHz, so we are now still in the strong coupling regime.

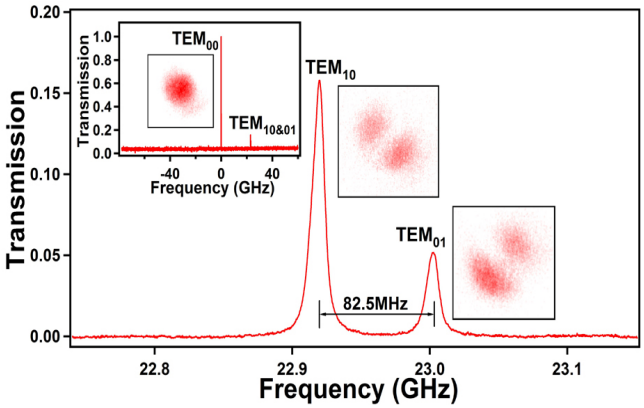

Figure 8. (Color online) When we scan the probe laser beam's detuning, the transmission signal vs the frequency detuning is recorded as shown by the red solid lines. The inset shows the resonance peaks of the TEM_{00}, TEM_{10} and TEM_{01} modes. The frequency splitting between the TEM_{10} and TEM_{01} modes is ~ 82.5 MHz. Three inset photos for the TEM_{00}, TEM_{10} and TEM_{01} modes' 2D intensity distributions are directly recorded by a CCD camera. Fortunately our mounted high-finesse micro-cavity has ~ 45-degree-tilted TEM_{10} and TEM_{01} modes.

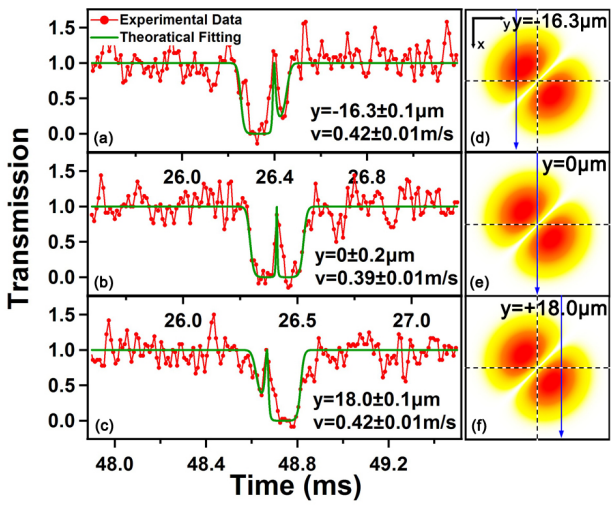

Figure 9. (Color online) The typical transmission signals (the red dots, as shown in the left column) measured by employing the ~ 45-degree-tilted TEM_{10} mode of our micro-cavity (as shown schematically in the right column) and the corresponding theoretical fittings (the green solid lines). The trajectories, $y \sim 16.3\ \mu m \pm 0.1\ \mu m$ for the case (a), $y \sim 0 \pm 0.2\ \mu m$ for the case (b), and $y \sim 18.0\ \mu m \pm 0.1\ \mu m$ are derived from the fittings.

Employing the strong coupling of individual free-fall atoms with the ~ 45-degree-tilted TEM_{10} mode of our micro-cavity, we determined motional trajectories of atoms inside the cavity [20]. Typical results are shown in Figure 9. As we expected, the degeneracy for determination of atomic trajectory is completely eliminated. The time bin for photon counting by the APD is set to 10 μs. The shorter time bin will decrease the signal-to-noise ratio. After analyzing more

results, we can estimate that the spatial resolution for determination of position y is ~ 0.1 μm in 10 μs [20]. The spatial resolution we achieved for position y is much better compared with previous works [21, 22].

For position z determination, actually in a relatively wide range, for example, from z = - 0.15 μm to +0.15 μm, our calculations show that the transmission signal drops down to almost zero. What we have observed is most likely in this range. When the position is too far from the range of - 0.15 μm < z < +0.15 μm, the fitting is getting worse due to the poor signal-to-noise ratio. So we do not choose those events beyond $z = \pm 0.15$ μm. Indeed it is very difficult to further distinguish different z inside the range of - 0.15 μm < z < +0.15 μm for one measured event, thus we could roughly estimate that the spatial resolution for position z determination is ~ 0.3 μm.

Furthermore, if we employ the higher-order transverse cavity mode, for example, the tilted TEM_{30} mode, as depicted in the right column in Figure 10, we expect to achieve better spatial resolution. For doing so, we simulated the corresponding cavity transmission spectra. The typical results are shown in the left column in Figure 10.

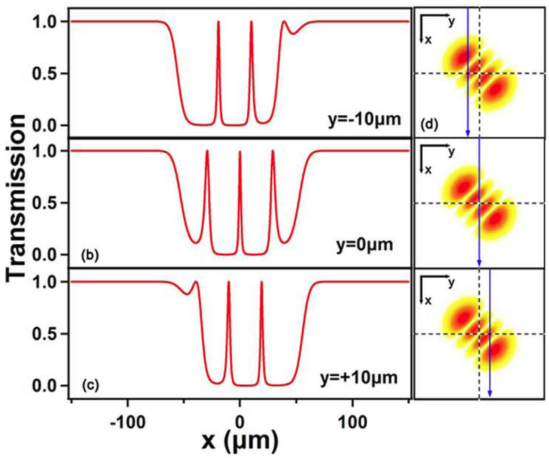

Figure 10. (Color online) If the single atom's trajectories are determined by employing the ~ 45-degree-tilted TEM_{30} cavity mode (as shown in the right column), the transmission signals (as shown schematically in the left column) are simulated for different trajectories, as the blue solid line with arrows shown in the right column. The higher-order cavity mode will help us to further improve the spatial resolution for determining the single atom's trajectories in side the cavity.

5. CONCLUSION

In conclusion, the strong coupling of single atoms with the TEM_{00} mode and the tilted TEM_{10} mode of a high-finesse FP-type micro-cavity has been realized in our cavity QED experiments with cold Cs atoms. For determining the effective temperature of cold atoms prepared in a MOT which located just above the cavity, the strong coupling of single atoms with the TEM_{00} cavity mode is employed to sensitively detect the individual free-fall atoms to obtain arrival times of atoms reaching the cavity mode. Also the strong coupling of single atoms with the TEM_{00} cavity mode is employed to track the atomic trajectory inside the cavity. But there is duplicate degeneracy due to the circle symmetry of TEM_{00} mode's intensity distribution. To improve the spatial resolution, the ~ 45-degree-tilted TEM_{10} mode of our high-finesse micro-cavity is employed to eliminate the duplicate degeneracy for the TEM_{00} mode and the horizon-oriented TEM_{10} mode, and also the fourfold degeneracy for the vertical-oriented TEM_{01} mode. The spatial resolution we achieved for position y determination is much better than previous works. Our technique could ultimately be applied to opto-mechanical cooling and time-resolved atom-cavity microscopy.

ACKNOWLEDGEMENT

This research work is supported by the National Natural Science Foundation of China (Grant Nos. 10794125, 60808006,

60978017, and 61078051), the National Major Scientific Research Program of China (Grant No. 2012CB921601), and the Project for Excellent Research Team of the National Natural Science Foundation of China (Grant No. 61121064).

REFERENCES

[1] H. J. Metcalf, H. J. and van der Straten, P., [Laser cooling and trapping], Springer-Verlag New York (1999).
[2] Berman, P., [Cavity quantum electrodynamics], Academic (1994).
[3] H. Mabuchi, Q. A. Turchette, M. S. Chapman, and H. J. Kimble, "Real-time detection of individual atoms falling through a high-finesse optical cavity," Opt. Lett. **21**, 1393-1395 (1996).
[4] Mabuchi, H., Ye, J., and Kimble, H. J., "Full observation of single-atom dynamics in cavity QED," Appl. Phys. B **68**, 1095-1108 (1999).
[5] Pinkse, P., Fischer, T., Maunz, P. and Rempe, G., "Trapping an atom with single photons," Nature **404**, 365-368 (2000).
[6] Ottl, A., Ritter, S., Kohl, M. and Esslinger, T., "Correlations and counting statistics of an atom laser," Phys. Rev. Lett. **95**, 090404 (2005).
[7] Teper, I., Lin, Y. and Vuletic, V., "Resonator-aided single-atom detection on a micro fabricated chip," Phys. Rev. Lett. **97**, 023002 (2006).
[8] Haase, A., Hessmo, B. and Schmiedmayer, J., "Detecting magnetically guided atoms with an optical cavity," Opt. Lett. **31**, 268-270 (2006).
[9] Poldy, R., Buchler, B. C. and Close, J. D., "Single-atom detection with optical cavities," Phys. Rev. A **78**, 013640 (2008).
[10] Zhang, P. F., Guo, Y. Q., Li, Z. H., Zhang, Y. C., Zhang, Y. F., Du, J. J., Li, G., Wang, J. M. and Zhang, T. C., "Temperature determination of cold atoms based on single-atom countings", J. Opt. Soc. Am. B **28**, 667-670 (2011).
[11] Chu, S., Hollberg, L., Bjorkholm, J. E., Cable, A. and Askin, A., "Three-dimensional viscous confinement and cooling of atoms by resonance radiation pressure," Phys. Rev. Lett. **55**, 48-51 (1985).
[12] Lett, P. D., Watts, R. N., Westbrook, C. I., Phillips, W. D., Gould, P. L. and Metcalf, H. J., "Observation of atoms laser cooled below the Doppler limit," Phys. Rev. Lett. **61**, 169-172 (1988).
[13] Kohns, P., Buch, P., Suptitz, W., Csambal, C. and Ertmer, W., "Online measurement of sub-Doppler temperatures in a Rb magneto-optical trap-by-trap centre oscillations," Europhys. Lett. **22**, 517-522 (1993).
[14] Walhout, M., Sterr, U., Orzel, C., Hoogerland, M. and Rolston, S. L., "Optical control of ultracold collisions in metastable Xenon," Phys. Rev. Lett. **74**, 506-509 (1995).
[15] Mitsunaga, M., Yamashita, M., Koashi, M. and Imoto, N., "Temperature diagnostics for cold sodium atoms by transient four-wave mixing," Opt. Lett. **23**, 840-842 (1998).
[16] Brzozowski, T. M., Maczynska, M., Zawada, M., Zachorowski, J. and Gawlik, W., "Time-of-flight measurement of the temperature of cold atoms for short trap-probe beam distances," J. Opt. B **4**, 62-66 (2002).
[17] Geng, T., Yan, S. B., Wang, Y. H., Yang, H. J., Zhang, T. C. and Wang, J. M., "Temperature measurement of cold atoms in a cesium magneto-optical trap by means of short-distance time-of-flight absorption spectrum," Acta Physica Sinica (Ch. Ed.) **54**, 5104-5108 (in Chinese) (2005).
[18] He, J., Wang, J., Qiu, Y., Wang, Y. H., Zhang, T. C. and Wang, J. M., "Influence of parameter errors on the temperature measurement of cold atoms via short-distance time-of-flight absorption spectra," Acta Physica Sinica (Ch. Ed.) **57**, 6221-6226 (in Chinese) (2008).
[19] Pradhan, S. and Jagatap, B. N., "Measurement of temperature of laser cooled atoms by one-dimensional expansion in a magneto-optical trap," Rev. Sci. Instr. **79**, 013101 (2008)
[20] Zhang, P. F., Guo, Y. Q., Li, Z. H., Zhang, Y. C., Zhang, Y. F., Du, J. J., Li, G., Wang, J. M. and Zhang, T. C., "Elimination of the degenerate trajectory of a single atom strongly coupled to a tilted TEM_{10} cavity mode," Phys. Rev. A **83**, 031804(R) (2011).
[21] Hood, C. J., Lynn, T. W., Doherty, A. C., Parkins, A. S. and Kimble, H. J., "The atom-cavity microscope: single atoms bound in orbit by single photons," Science **287**, 1447-1453 (2000).
[22] Puppe, T., Maunz, P., Fischer, T., Pinkse, P. W. H. and Rempe, G., "Single-atom trajectories in higher-order trans-verse modes of a high-finesse optical cavity," Phys. Scr. (Topical Issues) **T112**, 7-12 (2004).